Electrocatalysis

DOI: 10.1002/anie.201207517

Towards More Active and Stable Electrocatalysts for Formic Acid Electrooxidation: Antimony-Decorated Octahedral Platinum Nanoparticles**

*Francisco J. Vidal-Iglesias, Ana López-Cudero, José Solla-Gullón, and Juan M. Feliu**

Formic acid oxidation has been extensively studied on platinum, because it is considered a model electrocatalytic reaction for understanding fundamental aspects of electrocatalytic reactions. Its oxidation is generally accepted to take place through two parallel paths:[1] 1) direct oxidation to produce CO_2, and 2) a path mediated by a poison species, which consists of a dehydration step to yield water and adsorbed CO, followed by the oxidation of CO to CO_2 at high potentials. This latter path is undesirable for possible fuel cell applications. In the case of pure platinum, very low current densities are recorded in the positive-going sweep until poisoning CO is stripped off.[2] In earlier studies it was pointed out that the hysteresis between positive and negative-going voltammetric sweeps is due to the self-poisoning parallel path, which is also a structure-sensitive dehydration reaction.[1d] Experiments to determine the intrinsic activity of the different electrodes in the absence of poisoning have also demonstrated that direct oxidation is also structure sensitive and that the poisoning reaction is site-specific: a particular ensemble or junction of more than a single platinum site is required to dissociate formic acid.[3] In this way a possible electrocatalytic effect can be envisaged by the selective blocking of neighboring surface sites; this would lead to a distribution of isolated sites that are small enough to inhibit the poisoning step while still allowing the direct oxidation to take place. To achieve this purpose, foreign adatoms have been fruitfully used, not only on Pt single crystals, but also in practical electrocatalysts, such as shape-controlled Pt nanoparticles,[4] in which the influence of the surface structure can be understood.[5]

In the particular case of Sb-decorated Pt single crystals, some relevant features must be noted. When Sb is adsorbed onto Pt(100), the adatom produces a typical three-body effect by blocking surface sites and thus diminishing the number of locations in which CO can be formed from formic acid. As a consequence, the reactivity of the remaining isolated sites reaches values similar to those corresponding to the intrinsic activity of the Pt(100) surface.[6] Also, the voltammetric peak potential takes place in the same potential range, which suggests that no other special electronic effects are caused by the presence of Sb on the Pt surface. Similar effects have been described at the Pt(110) electrode.[6] However, a different situation is observed when Sb is adsorbed onto Pt(111) surfaces. In this case, a strong inhibition of poisoning is observed, even with low coverage of the adatom, thus discarding the role of three-body ensemble effects. Moreover, oxidation takes place at significantly lower potentials when the surface is covered by Sb. This points to a true modification of surface reactivity, resulting in a more active catalyst than Pt(111)[7] at low potentials. Moreover, formic acid oxidation does not require oxygen species in the direct path and consequently a possible bifunctional-mechanism effect can be ruled out. However, if some CO could be formed by the indirect path, the oxidized Sb adatoms could also have an electrocatalytic effect through a bifunctional mechanism.[7]

Herein we present the preparation and electrochemical characterization of Sb-decorated Pt nanoparticles with a preferential (111) surface structure. We compare the reactivity of Sb-modified octahedral Pt nanoparticles ($Sb/Pt_{octahedral}$) and their enhanced activity towards formic acid electrooxidation with that of cubic and spherical nanoparticles (synthetic details are given in the Supporting Information).

Figure 1 A shows formic acid electrooxidation for the octahedral nanoparticles before and after Sb adatom decoration. As can be seen adatom adsorption enhances HCOOH oxidation, especially at low potentials, where the oxidation current is strongly inhibited on bare octahedral nanoparticles. In Figure 1 B the voltammetric behavior of the three different types of nanoparticles employed in this reaction is compared. Octahedral nanoparticles, which are enriched in sites with (111) geometry, show the highest activity, followed by spherical nanoparticles, and then the cubic nanoparticles, which are enriched in (100) geometry sites, are the least active of the Sb-decorated surfaces tested. These results are based on samples possessing the Sb decoration that provides the highest activity of each Sb-modified sample. The results obtained can be explained in terms of the effect of the specific surface structure of each Pt nanoparticle. The low potential region deserves special attention because of the new contribution that appears around 0.18 V in both the positive and negative scans when Sb is incorporated onto the surface of the octahedral nanoparticle. For a Pt(111) electrode (an octahedron is ideally enclosed by eight (111) faces), the presence of a shoulder in the positive scan at 0.18 V has been ascribed to

[*] Dr. F. J. Vidal-Iglesias, Dr. A. López-Cudero, Dr. J. Solla-Gullón, Prof. J. M. Feliu
Institute of Electrochemistry, University of Alicante
Apartado 99, 03080 Alicante (Spain)
E-mail: juan.feliu@ua.es
Homepage: http://web.ua.es/en/eqsup

[**] This work has been financially supported by the MICINN (Feder) of Spain and the Generalitat Valenciana through projects CTQ2010-16271 and PROMETEO/2009/45. F.J.V.I. also thanks the European Social Funding.

Supporting information for this article is available on the WWW under http://dx.doi.org/10.1002/anie.201207517.

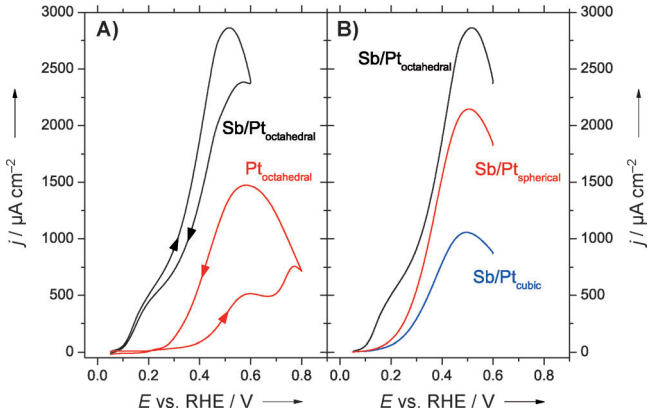

Figure 1. A) Voltammetric profiles for the electrooxidation of formic acid with bare (red line) and Sb-decorated (black line) octahedral nanoparticles. B) Positive-sweep voltammetric profiles for the electrooxidation of formic acid with octahedral (black line), polyoriented (red line) and cubic (blue line) Sb-decorated platinum nanoparticles. Test solution consisted of H_2SO_4 (0.5 M) and HCOOH (0.1 M). Sweep rate = 20 mV s^{-1}.

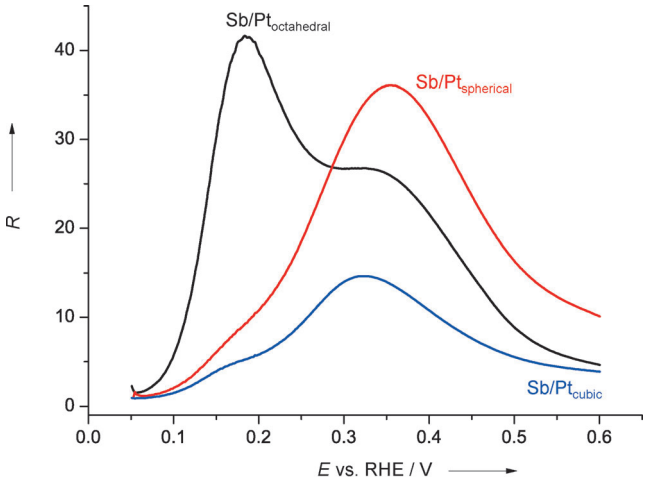

Figure 2. Potential dependence of the enhancement factor (R), which is defined as the current density of the Sb-decorated shaped nanoparticles with the optimum coverage over that of the corresponding unmodified nanoparticles for the positive scan. Test solution consisted of H_2SO_4 (0.5 M) and HCOOH (0.1 M). Sweep rate = 20 mV s^{-1}.

the formation of a Sb–Pt alloy, probably by place exchange with the surface Pt atoms.[7] Interestingly, this shoulder was neither observed for the other two platinum basal planes, Pt(110) or Pt(100), nor for stepped surfaces such as Pt(320) and Pt(331).[6] For this latter electrode, which consists of three-atom-wide (111) terraces and (111) monoatomic steps, formic acid oxidation was also enhanced by Sb decoration. Moreover, the absence of oxidation current at low potential demonstrates the importance of the presence of wide terraces with (111) geometry. Therefore, with regards to the current density obtained at 0.2 V in the positive scan, octahedral nanoparticles show a 5 and an 8-fold increase versus the spherical and cubic nanoparticles, respectively. Direct comparison with the bare octahedral nanoparticles is meaningless, as there is no significant oxidation at that potential, which already suggests the importance of Sb-decoration for fuel cell applications.

Figure 2 shows the enhancement factor (R) reported for voltammetric studies, which is defined as the ratio between the current densities of the Sb-decorated nanoparticles (with optimum coverage) versus that of the corresponding unmodified nanoparticles, both in the positive scan. This ratio varies with the applied potential and depends on the shape of the nanoparticles. For the octahedral nanoparticles, the maximum ratio is observed at approximately 0.18 V, which corresponds to the previously described shoulder. The octahedral nanoparticles not only give the highest R value, but also at lower potentials than the other samples, making this combination promising from the application point of view. In fact, as previously shown with model Pt surfaces, CO can be oxidized on Sb-modified Pt(111) single crystals at much lower potentials than for bare Pt(111), and poison formation is almost completely suppressed at very low Sb coverages (ca. 0.03 monolayers),[7] which explains the high catalytic activity reported for the octahedral nanoparticles.

Figure 3 shows the effect of the progressive increase of Sb coverage on the surface of the octahedral Pt nanoparticles.

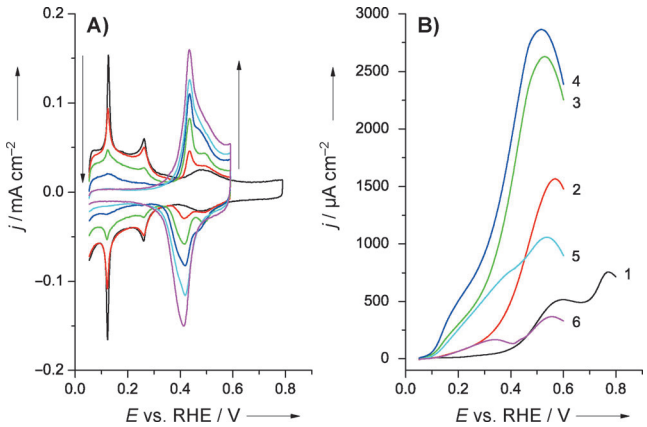

Figure 3. Voltammetric profile for octahedral nanoparticles decorated with increasing amounts of Sb in H_2SO_4 (0.5 M) in the absence (A) and presence (B) of HCOOH (0.1 M). Increasing amounts of Sb are indicated by an arrow in (A) and with increasing numbers in (B), where 1 corresponds to bare octahedral Pt nanoparticles. Sweep rate = 50 mV s^{-1} for (A) and 20 mV s^{-1} for (B).

The increasing amount of Sb decorating the surface can be correlated with a decrease in the hydrogen adsorption/desorption region, Figure 3 A. Furthermore, a redox peak from the presence of Sb appears and continues to grow, even when the hydrogen adsorption region is completely blocked. For the same decorated surfaces, Figure 3 B shows the corresponding voltammetric profile for formic acid oxidation. These results indicate that there is a maximum in activity after which further incorporation of Sb leads to a less active surface, owing to the full blocking of the active sites on the platinum surface.

A deeper analysis of the results as a function of Sb coverage is required. Its calculation at low coverage can be followed by the decrease of the hydrogen adsorption/desorption region. However, this method loses precision at high coverage (close to the monolayer), as in our case, and a better

method is necessary. For this purpose, the charge of the hydrogen desorption region was plotted versus the charge of the Sb oxidation peak. From this plot, the charge of Sb that corresponds to a monolayer was obtained through extrapolation to $Q_H = 0$ (see the Supporting Information for further details). A Q_{Sb} value of $182 \pm 18\ \mu C\,cm^{-2}$ was found for the different samples. This value is very close to those reported for different Pt single crystals.[6,7]

Chronoamperometric experiments were also performed to evaluate the time-dependent activity of the Sb decorated samples. Figure 4A shows the current densities recorded after

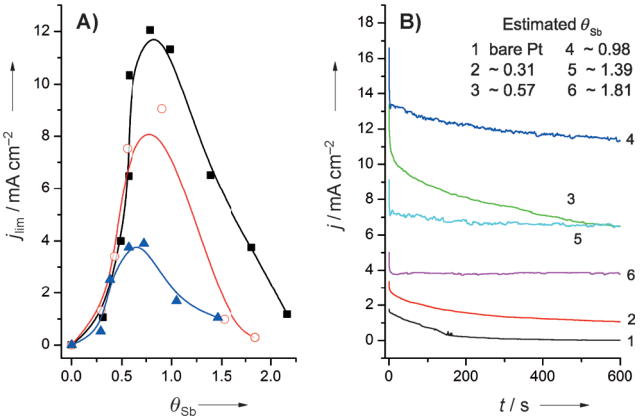

Figure 4. A) Current densities after 10 min at 0.2 V for $Sb/Pt_{octahedral}$ (solid squares), $Sb/Pt_{spherical}$ (open circles) and Sb/Pt_{cubic} (solid triangles) platinum nanoparticles. B) Chronoamperometric curves for $Sb/Pt_{octahedral}$ nanoparticles for increasing θ_{Sb}. Test solution consisted of H_2SO_4 (0.5 M) and HCOOH (1 M).

10 min at a potential value as low as 0.2 V for the $Sb/Pt_{octahedral}$, $Sb/Pt_{spherical}$ and Sb/Pt_{cubic} nanoparticles. As in the voltammetric experiments, there is an optimum coverage, ranging between $0.65 < \theta_{Sb} < 0.80$ for the different samples. In terms of current stability, some other important features have to be noted. Independent of the sample (Figure 4B shows octahedral nanoparticles, see the Supporting Information for other samples), once the optimum Sb coverage is reached the time-dependent activity becomes very stable, although at the expense of lower current densities, in comparison with the optimal coverage.

To better illustrate this deactivation rate, Table 1 summarizes the current densities obtained at two different times (1 min and 10 min). In all cases, a catalyst with optimum Sb coverage has been used to extract the data; for the $Sb/Pt_{octahedral}$ nanoparticles, data for three different coverages are given (the optimum and two with higher coverages). Remarkably, a very low deactivation value of only about 1% can be achieved in some cases. These values are much lower than those previously reported for Pd-decorated Pt nanoparticles, for which a deactivation of about 80% was also observed after 10 min.[4c]

In summary, we have demonstrated how better electrocatalysts can be designed for formic acid fuel cells by the specific control of electrocatalyst surface structure/shape and specific adatom decoration. A similar strategy can be followed for different reactions, profiting from the previous knowledge gained from adatom-decorated Pt single crystal studies.

Table 1: Current densities after 1 and 10 min at 0.2 V, and deactivation[a] for Sb-decorated platinum nanoparticles.[b]

Catalyst[c]	$j_{1\,min}$ [mA cm^{-2}]	$j_{10\,min}$ [mA cm^{-2}]	Deactivation [%]
$Sb/Pt_{octahedral}$ (4)	12.90	11.30	12
$Sb/Pt_{octahedral}$ (5)	7.07	6.51	8
$Sb/Pt_{octahedral}$ (6)	3.79	3.75	1
Sb/Pt_{cubic}	5.18	4.23	18
$Sb/Pt_{spherical}$	10.10	9.04	10

[a] Deactivation is defined as $[(j_{1\,min} - j_{10\,min})j_{1\,min}^{-1}]$. [b] Test solution consisted of H_2SO_4 (0.5 M) and HCOOH (1 M). [c] Numbers in parentheses refer to the corresponding curve in Figure 4B.

Experimental Section

The experimental details for the synthesis and cleaning of Pt nanoparticles are included in the Supporting Information. All electrochemical measurements were performed at room temperature and electrolyte solutions were prepared from Milli-Q® water and Merck p.a. sulfuric and formic acids. A three-electrode electrochemical cell was used. The electrode potential was controlled using a PGSTAT30 AUTOLAB system. The counter electrode used was a gold wire. Potentials were measured against a reversible hydrogen electrode (RHE) connected to the cell through a Luggin capillary. Before each experiment, the gold collector was mechanically polished with alumina and rinsed with ultra-pure water to eliminate the nanoparticles from previous experiments. The active surface area of the Pt nanoparticles was determined by the charge involved in the hydrogen UPD region (between 0.05 V and 0.65 V) assuming $0.23\ mC\,cm^{-2}$ for the total charge after the subtraction of the double layer charging contribution.[8] The estimation of Sb coverage is included in the Supporting Information.

Received: September 17, 2012
Published online: November 23, 2012

Keywords: antimony · electrocatalysis · nanoparticles · oxidation · platinum

[1] a) A. Capon, R. Parsons, *J. Electroanal. Chem.* **1973**, *44*, 239–254; b) A. Capon, R. Parsons, *J. Electroanal. Chem.* **1973**, *44*, 1–7; c) N. M. Markovic, P. N. Ross, *Surf. Sci. Rep.* **2002**, *45*, 117–229; d) J. M. Feliu, E. Herrero in *Handbook of Fuel Cells—Fundamentals, Technology and Applications*, *Vol. 2* (Eds.: W. Vielstich, H. Gasteiger, A. Lamm), Wiley, Chichester, **2003**.

[2] a) H. Kita, H. W. Lei, *J. Electroanal. Chem.* **1995**, *388*, 167–177; b) T. Iwasita, X. H. Xia, E. Herrero, H. D. Liess, *Langmuir* **1996**, *12*, 4260–4265.

[3] a) V. Grozovski, V. Climent, E. Herrero, J. M. Feliu, *ChemPhysChem* **2009**, *10*, 1922–1926; b) V. Grozovski, V. Climent, E. Herrero, J. M. Feliu, *Phys. Chem. Chem. Phys.* **2010**, *12*, 8822–8831.

[4] a) E. Leiva, T. Iwasita, E. Herrero, J. M. Feliu, *Langmuir* **1997**, *13*, 6287–6293; b) L. A. Kibler, A. M. El-Aziz, R. Hoyer, D. M. Kolb, *Angew. Chem.* **2005**, *117*, 2116–2120; *Angew. Chem. Int. Ed.* **2005**, *44*, 2080–2084; c) F. J. Vidal-Iglesias, J. Solla-Gullon, E. Herrero, A. Aldaz, J. M. Feliu, *Angew. Chem.* **2010**, *122*, 7152–7155; *Angew. Chem. Int. Ed.* **2010**, *49*, 6998–7001; d) J. Rossmeisl, P. Ferrin, G. A. Tritsaris, A. U. Nilekar, S. Koh, S. E. Bae, S. R.

Brankovic, P. Strasser, M. Mavrikakis, *Energy Environ. Sci.* **2012**, *5*, 8335 – 8342.
[5] a) N. Tian, Z. Y. Zhou, S. G. Sun, *J. Phys. Chem. C* **2008**, *112*, 19801 – 19817; b) M. T. M. Koper, *Nanoscale* **2011**, *3*, 2054 – 2073; c) J. Solla-Gullón, F. J. Vidal-Iglesias, J. M. Feliu, *Annu. Rep. Prog. Chem. Sect. C* **2011**, *107*, 263 – 297.
[6] Y.-Y. Yang, S.-G. Sun, Y.-J. Gu, Z.-Y. Zhou, C.-H. Zhen, *Electrochim. Acta* **2001**, *46*, 4339 – 4348.
[7] V. Climent, E. Herrero, J. M. Feliu, *Electrochim. Acta* **1998**, *44*, 1403 – 1414.
[8] Q. S. Chen, J. Solla-Gullon, S. G. Sun, J. M. Feliu, *Electrochim. Acta* **2010**, *55*, 7982 – 7994.

